Experimental Mechanics (2010) 50:1235–1243
DOI 10.1007/s11340-009-9325-7

Energy Emissions from Failure Phenomena: Mechanical, Electromagnetic, Nuclear

A. Carpinteri · F. Cardone · G. Lacidogna

Received: 3 December 2009 / Accepted: 21 December 2009 / Published online: 26 January 2010

Abstract Characterizing the nature of the different forms of energy emitted during compressive failure of brittle materials is an open and debated argument in the scientific literature. Some research has been already conducted on this subject in the scientific community based on the signals captured by the acoustic emission measurement systems. On the other hand, there are not many studies yet about the emission of electromagnetic charge, and for the first time we are talking about piezonuclear neutron emissions from very brittle failure of rocks specimens in compression. The authors analyze these three different emissions from an experimental point of view.

Keywords Brittle failure · Acoustic emission · Electromagnetic emission · Neutron measurements · Piezonuclear reactions · Element evolution

Presented at the SEM-2009 Conference, Albuquerque NM, USA, June 1st, 2009.

A. Carpinteri (✉, SEM member) · G. Lacidogna (SEM member)
Department of Structural Engineering & Geotechnics,
Politecnico di Torino,
Corso Duca degli Abruzzi 24,
10129 Torino, Italy
e-mail: alberto.carpinteri@polito.it

G. Lacidogna
e-mail: giuseppe.lacidogna@polito.it

F. Cardone
Istituto per lo Studio dei Materiali Nanostrutturati (ISMN-CNR),
Via dei Taurini 19,
00185 Roma, Italy
e-mail: fabio.cardone@ismn.cnr.it

Introduction

It is possible to demonstrate experimentally that the failure phenomena, in particular when they occur in a brittle way, i.e. with a mechanical energy release, emit additional forms of energy related to the fundamental natural forces.

While the acoustic emission (AE), due to pressure waves travelling in the medium as it happens for earthquakes, is well-known and already exploited for monitoring purposes, the electromagnetic radiation (EM), due to an electric charge redistribution after material failure, can be considered a relatively new phenomenon, which is at present under investigation. As regards, then, the neutron emission, this is the first time that a similar phenomenon is captured [1, 2].

Only for fluids subjected to cavitation, analogous piezonuclear emissions of neutrons were previously found in the experiments. Totally accepted theories explaining such anomalous phenomena are still lacking in the literature. It is not in the aims of the present contribution to provide a theoretical physics explanation to piezonuclear emissions, although the emergence of these emissions in relation to a cusp catastrophe failure may result to be of interest also to Experimental Mechanics.

Acoustic Emission

A Fractal Criterion for AE Monitoring

Monitoring a structure by means of the AE technique, it proves possible to detect the occurrence and evolution of stress-induced cracks. Cracking, in fact, is accompanied by the emission of elastic waves which propagate within the bulk of the material. These waves can be received and recorded by transducers applied to the surface of structural

elements. This technique, originally used to detect cracks and plastic deformations in metals, has been extended to studies in the field of rocks and can be used for the diagnosis of structural damage phenomena [3].

In AE monitoring, piezoelectric (PZT) sensors are generally used, thereby exploiting the capabilities of certain crystals to produce electric signals whenever they are subjected to a mechanical stress. The signal picked up by a transducer is preamplified and transformed into electric voltage (Fig. 1). It is then filtered to eliminate unwanted frequencies, such as the vibration arising from the mechanical instrumentation, which is generally lower than 100 kHz. Up to this point the signal can be represented as a damped oscillation. The signal is therefore analysed by a measuring system counting the emissions that exceed a certain voltage threshold measured in volts (V).

Recently AE data have been interpreted by the authors on the basis of the statistical and fractal theories of fragmentation [4–6]. The following *size-scaling* law is assumed during the damage process:

$$W \propto N \propto V^{D/3}, \tag{1}$$

where W is the released energy, V the structural element volume, D the so-called fractal exponent comprised between 2 and 3, and N the cumulative number of AE events that the structure provides during the damage monitoring. The damage level of a structure can be obtained from AE data of a reference specimen (pedex r) extracted from the structure itself and tested up to failure. From equation (1) we have:

$$N_{\max} = N_{\max r}(V/V_r)^{D/3}, \tag{2}$$

from which we can obtain the critical number of acoustic emission events $N_{\max}$ that the structure may provide before achieving the critical condition. The details of the procedure are given in references [7].

The authors have also shown that energy release, as measured with the AE technique during the damaging process, obey the following *time-scaling* law [7, 8]:

$$W \propto N \propto t^{\beta_t}, \text{ with } 0 \le \beta_t \le 3, \tag{3}$$

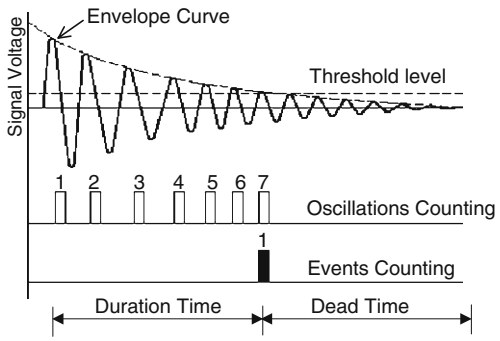

Fig. 1 Schematic signal detected by AE technique

where t is the monitoring time and β_t stands for the time-scaling exponent of the released energy. The experimental validation of equation (3) was carried out through laboratory compressive tests conducted on concrete cylinders of different diameters and slenderness ratios. All compressive tests were performed under displacement control, by imposing a constant rate to the upper loading platen. The trend observed was that of an increase in β_t with increasing specimen diameter. The *time-scaling* values obtained experimentally were seen to agree with the law of equation (3), providing an exponent in the range 1.38 to 2.92 [8].

Using the AE monitoring technique, we have analysed the evolution of cracks and estimated the released strain energy during their propagation in structural members. Significant tests were performed on laboratory specimens and full-size structures [7].

Experimental Results for the Fractal Exponent D

Laboratory tests were performed on the cylindrical concrete specimens in compression, shown in Fig. 2(a), to obtain an experimental confirmation of the laws described above [7, 8]. A comparison between experimental results and theoretical predictions is herein presented. For all the tested specimens, the critical number of acoustic emissions $N_{\max\ r}$ was evaluated in correspondence to the peak stress σ_u. The compression tests show an increase in AE cumulative event number by increasing the specimen volume. Subjecting the average experimental data to a statistical analysis, we can quantify the parameters D in equation (1). The parameter D represents the slope, in the bilogarithmic diagram, of the line that relates $N_{\max}$ to the specimen volume. From the best-fitting, we obtain $D/3 \cong 0.766$, Fig. 2(b), so that the fractal exponent results, as predicted by the fragmentation theories, to be comprised between 2.0 and 3.0 ($D \cong 2.3$).

AE Frequency-magnitude Statistics

Extensive studies on fracture of brittle materials by means of the AE technique have shown that fracture and damage growth can be characterized through the b-value of the Gutenberg-Richter (GR) law, which changes systematically during the different stages of the failure process. This parameter can be linked to the value of the exponent of the power-law distribution of the crack size in a damaged medium. We propose a statistical interpretation for the variation of the b-value during the evolution of damage detected by AE, which is based on a treatment originally proposed by Carpinteri and co-workers [9–12]. The proposed model captures the transition from the condition of diffused criticality to that of imminent failure localisation.

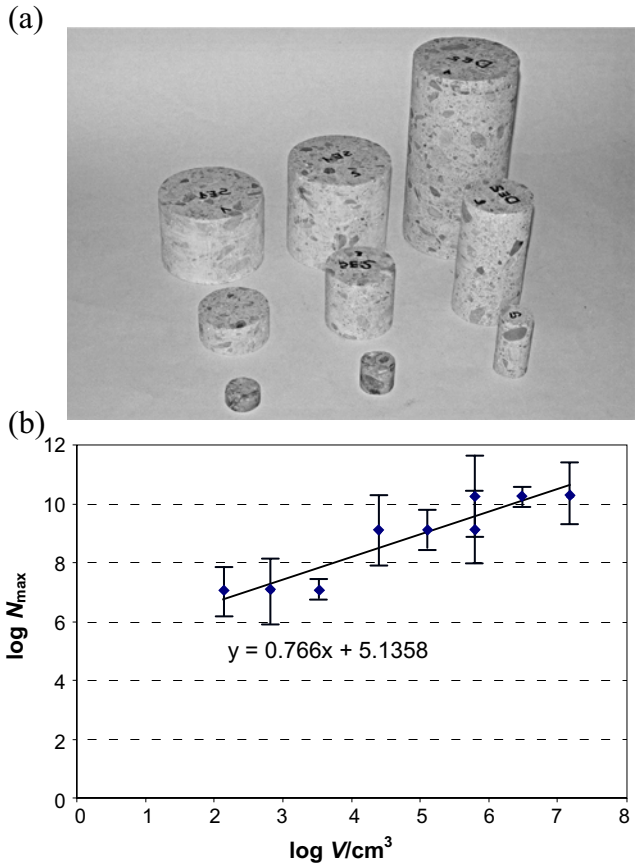

Fig. 2 (**a**) Geometries of the tested specimens. (**b**) Volume-effect on N_{max}

According to seismology [13], the magnitude in terms of AE technique is defined as follows:

$$m = Log_{10}A_{\max} + f(r), \tag{4}$$

where A_{max} is the signal amplitude, measured in volts, while $f(r)$ is a correction taking into account that the amplitude is a decreasing function of the distance r between the source and the sensor. According to Uomoto [14], for large-sized structures, the amplitude reduction for AE signals is $f(r)=k\ r$, where r is measured in meters and k is equal to five magnitudes per meter. Signal amplitude analyses must be performed by means of an AE equipment that can identify the complete shape of AE waves [15].

In seismology, earthquakes of larger magnitude occur less frequently than earthquakes of smaller magnitude. This fact can be quantified in terms of a magnitude-frequency relation, proposed by Gutenberg and Richter in an empirical way:

$$Log_{10}N(\geq m) = a - bm, \text{ or } N(\geq m) = 10^{a-bm}, \tag{5}$$

where N is the cumulative number of earthquakes with magnitude $\geq m$ in a specified area and over a specified time span, and a and b are positive constants varying from region to region.

The GR relationship has been tested successfully in the acoustic emission field to study the scaling of the "amplitude distribution" of AE waves [11, 12, 16]: this approach substantiates the similarity between the damage process in a structure and the seismic activity in a region of the Earth Crust and, at the same time, it widens the scope of the GR relationship. From equation (5), we find that the b-value is the negative gradient of the log-linear AE frequency-magnitude diagram and hence it represents the slope of the amplitude distribution. The b-value changes systematically during the different stages of damage growth [11, 12, 16], and hence it can be used to estimate the development of the damage process.

b-value Analysis

The aim is to establish a theoretical basis for taking $b_{min}=1.0$ at failure, as observed both in AE laboratory tests and in tests performed on full sized engineering structures [9–12]. By analogy with earthquakes, the AE damage *size-scaling* entails the validity of the relationship:

$$N(\geq L) = cL^{-2b}, \tag{6}$$

where N is the cumulative number of AE events generated by source defects with a characteristic linear dimension $\geq L$, c is a constant of proportionality, and $2b=D$ is the fractal dimension of the damage domain [17, 18]. It has been pointed out that this interpretation rests on the assumption of a dislocation model for the seismic source and requires that $2.0 \leq D \leq 3.0$, i.e., the cracks are distributed in a fractal domain comprised between a surface and the volume of the analysed region [17, 18].

The cumulative distribution (6) is substantially identical to the cumulative distribution proposed by Carpinteri [9, 10], which gives the probability of a defect with size $\geq L$ being present in a body:

$$P(\geq L) \propto L^{-\gamma}. \tag{7}$$

Therefore, the number of defects with size $\geq L$ is:

$$N^*(\geq L) \sim N_{tot}L^{-\gamma}, \tag{8}$$

where γ is a statistical exponent measuring the degree of disorder, i.e. the scatter in the defect size distribution, and N_{tot} is the total number of defects in the body. By equating distributions (6) and (8) it is found that: $2b=\gamma$.

At the collapse, the size of the maximum defect is proportional to the characteristic size of the structure. As shown in [10–12], the related cumulative defect size distribution (referred to as self-similarity distribution) is characterized by the exponent $\gamma=2.0$, which corresponds to $b=1.0$. In [10] it was also demonstrated that $\gamma=2.0$ is a lower bound which corresponds to the minimum value $b=$

1.0, observed experimentally when the load bearing capacity of a structural member has been exhausted.

Therefore, by determining the b-value it is possible to identify the modalities of energy dissipation in a structural element during the monitoring process. The extreme cases envisaged by equation (1) are D=3.0, which corresponds to the critical conditions b=1.5, when energy dissipation takes place through small defects homogeneously distributed throughout the volume, and D=2.0, which corresponds to b=1.0, when energy dissipation takes place on a surface. In the former case diffused damage is observed, whereas in the latter two-dimensional cracks are formed leading to the separation of the structural element.

Experimental Results on b-value

From the laboratory tests described above, one of the 59 mm diameter specimens, with a height/diameter ratio h/d=2, is shown in Fig. 3(a) [15]. The compression tests were performed in displacement control, by imposing a constant rate of displacement to the upper loading platen. A displacement rate equal to 4×10^{-6} m/s was adopted to obtain a slow crack growth. Compressive load vs. time, cumulated event number, and event rate for each second of the testing period are depicted in Fig. 3(b). The load-time diagram was subdivided into three stages. A first stage (t_0, t_1) extending from the initial time to peak load, a second stage (t_1, t_2) going from peak load to the mainshock, as identified by the maximum value of the acoustic emission rate, and a third stage (t_2, t_f) going from the mainshock to the end of the process. The b-values obtained for each stage are shown in Fig. 3(c); they range from 1.64 to 1.20. The minimum value, rather close to 1.0, was obtained in the softening tail of the load-time curve.

These values are in good agreement with the fractal laws, equations (6) and (8). At the start of the loading process, energy dissipation takes place mostly through the formation of microcracks scattered throughout the volume of the material ($b \cong 1.64$, $D \cong 3.0$); at the end of the process, instead, energy dissipation is seen to concentrate

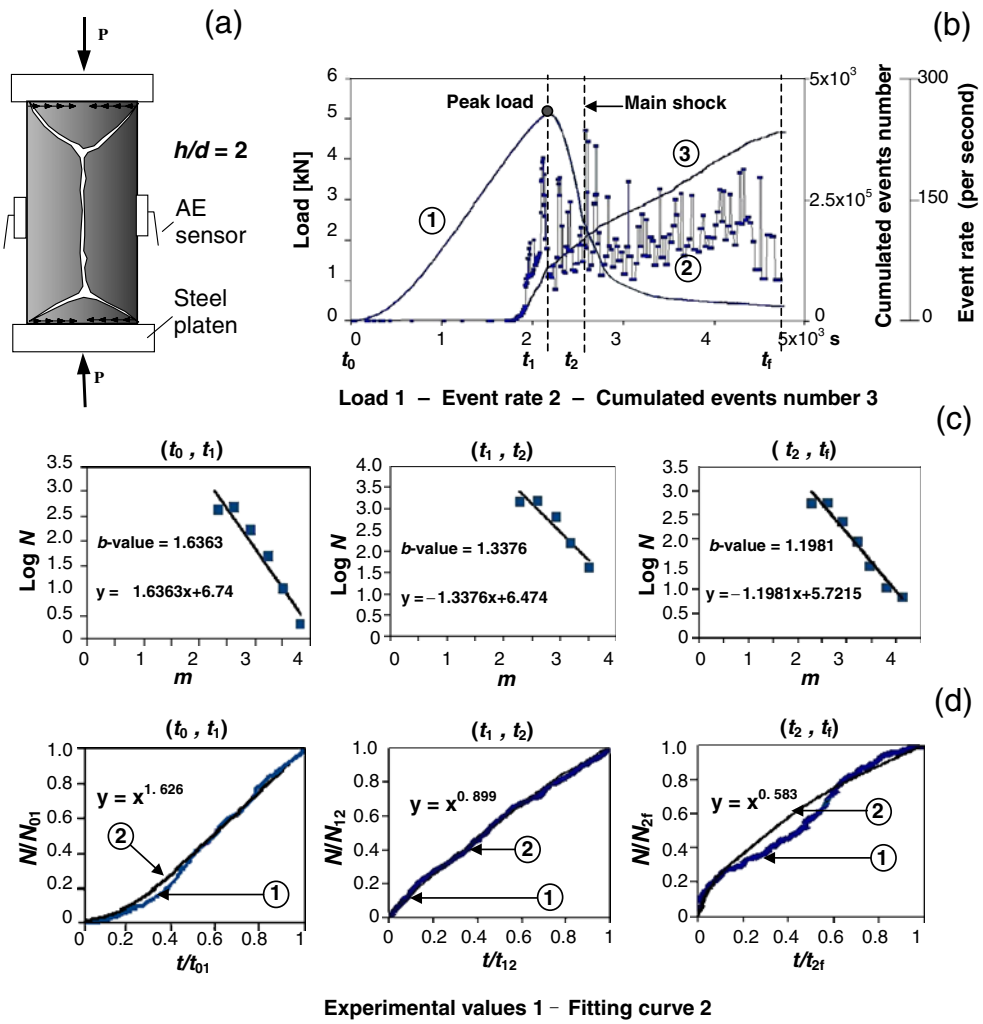

Fig. 3 Cylindrical concrete specimen in compression. (**a**) Testing set-up. (**b**) Load vs. time curve and AE activity. (**c**) b-values during the test. (**d**) Variation in β_t parameter during the test

into a two-dimensional crack of a size comparable to that of the specimen, which brings about its separation ($b \cong 1.20$, $D \cong 2.0$).

The initial and final values presented by the fractal exponent D, obtained through the b-values, are strictly connected to the analogous exponent evaluated on the basis of the fragmentation theories: $D \cong 2.3$, see Fig. 2(b). The latter, indeed, is related to the critical cumulative number of acoustic emissions N_{max} at the peak stress σ_u, when the crack formation is not yet so advanced to lead to the complete specimen separation.

The non-perfect matching between the values of D exponent at the peak load, obtained by equation (1) and b-value procedures, is due to the fact that both are indirect estimations of the fractal dimension D. As a matter of fact, equation (1) evaluates D by an energetic approach, while the b-value is based on a statistical model, that in this case overestimates the D exponent [Fig. 3(c)]. The direct computation of the fractal dimension D should be performed by geometrical methods like box-counting [18], which need the exact localization of AE sources.

In conclusion, taking into account available AE data — event counts, event magnitudes, event source localization— we can apply one or more of these procedures to get the fractal dimension of the damage domain.

Finally, for the three loading stages, Fig. 3(d) gives the values of the β_t parameter, equation (3). The values, between 1.63 and 0.58, were determined by best-fitting the cumulating count of the AE events divided by the total count for each loading stage. These results confirm that during the sequences of signals preceding the critical condition (foreshock), it is $\beta_t > 1$, whereas during the sequences following the critical condition (aftershock),$\beta_t < 1$, energy dissipation having been exhausted. It should be noted that a comparative reading of the b-value and β_t parameter makes it possible to assess the evolution of the entire loading process: the β_t parameters, in fact, have a *predictive* function relative to the reaching of the critical condition, whereas the b-values have a *descriptive* function relative to the damage level reached.

Electromagnetic Emission

It is reported in the literature that changes in geoelectric potential and anomalous radiation of geoelectromagnetic waves, especially in low-frequency bands, occur before major earthquakes. At the laboratory scale, similar phenomena have also been observed on rock specimens under compression tests [19]. In this case, crack growth is accompanied by acoustic emission ultrasonic waves (AE) and electromagnetic emission (EME). We measured the magnetic field, given by the moving charges, in the low-frequency range (from 10 Hz to 400 kHz) during laboratory fracture experiments on rocks and concrete samples loaded up to failure [20].

Four specimens made of different brittle materials, Concrete, Syracuse Limestone, Carrara Marble and Green Luserna Granite, were examined in this study. The acoustic emission emerging from the compressed specimens was detected applying to the sample surface a PZT transducer, sensitive in the frequency range from 50 to 500 kHz, for detection of AE. By means of PZT accelerometric transducers, we have also identified AE at low frequencies (between 1 kHz and 10 kHz) emerging just before the collapse of the Concrete specimen [21]. The EM emission was analysed using an isotropic probe calibrated for measuring magnetic fields. The adopted device works in the frequency range between 10 Hz and 400 kHz, the measurement range is between 1 nT to 80 mT, and the three-axial measurement system has a 100 cm^2 magnetic field sensor for each axis. This device was placed 1 m away from the specimens.

In all the considered cases, the presence of AE events has been always observed during the damage process. On the contrary, it is very interesting to note that, despite their different mechanical behaviour, all the specimens generate EME only during sharp drops in stress. These sharp stress drops are due to a rapid decay of the material mechanical properties, generated by the formation of new micro-cracks during the loading process. Indeed, as has been shown, the energy release modalities during compressive tests depend on the intrinsic brittleness of the material of the test specimens, as well as on test specimen dimensions and slenderness [22–24].

One of the experiments conducted on a rock specimen, Syracuse Limestone, is depicted in Fig. 4. The specimen was subjected to uniaxial compression by imposing a displacement rate of 1×10^{-6} m/s to obtain a very slow crack growth. As can be seen in Fig. 4, the mechanical behaviour of the specimen is characterized by a complex load vs. time diagram. This is due to the composition of limestone, which is a natural and heterogeneous material. We observed a constant increase in AE until the first stress drop, occurred at 70% of the peak load. This stage is followed by a staircase response up to the peak load. The cumulated number of AE events saturates after the peak load. Three EME events, with magnetic fields ranging between 1.4 and 1.8 μT, were detected in correspondence of each observed stress drop until the peak load was reached.

Even in this case, AE plays the role of fracture precursor since it precedes EME events accompanying stress drops and related discontinuous fracture advancements. During the post-peak stage, i.e., softening branch in the load vs. time diagram, no further EME signals were detected. In fact, at the peak load the fracture is completely formed and

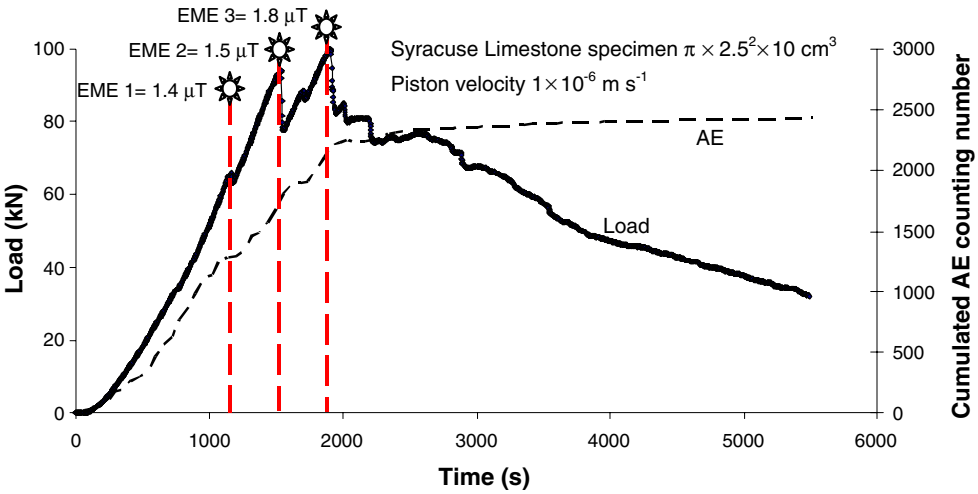

Fig. 4 Load vs. time curve of the Syracuse Limestone specimen (*bold line*). The dashed line represents the cumulated number of AE. The stars on the graph show the moments of EME events with magnetic fields comprised between 1.4 and 1.8 μT

the subsequent stages are characterized mainly by opening of the fracture surfaces.

This evidence enables the simultaneous investigation of AE and EM signals as collapse precursors in materials like rocks and concrete. Furthermore, the observed magnetic activity from laboratory experiments looks very promising for effective applications at the geophysical scale [19].

Piezonuclear Emission

Neutron emission measurements by means of helium-3 neutron detectors were performed on rock test specimens during crushing failure [1, 2].

Experimental data from rocks tested in compression generally indicate that this is a brittle material, since it exhibits a rapid decrease in load carrying capacity when deformed beyond a peak load. When the softening diagram is very steep, or even shows simultaneously decreasing strain and stress values, the material is said to present a snap-back or catastrophic behaviour. This is in contrast with ductile materials which retain considerable strength beyond the peak as shown in Fig. 5 [22–24].

The materials selected for the compression tests were Carrara Marble (calcite) and green Luserna Granite (gneiss). This choice was prompted by the consideration that they present a different iron content and, test specimen dimensions being the same, different brittleness numbers [22] would cause catastrophic failure in granite, not in marble. The test specimens were subjected to uniaxial compression to assess scale effects on brittleness [23]. Four test specimens were used, two made of Carrara Marble, consisting mostly of calcite, and two made of Luserna Granite, all of them measuring $6\times6\times10$ cm^3.

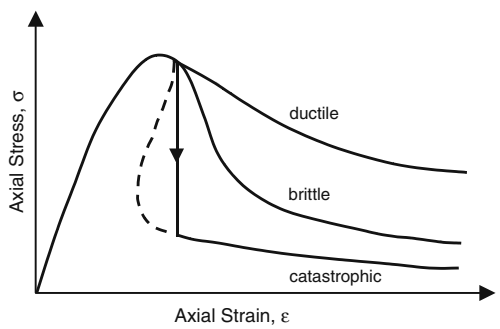

Fig. 5 Ductile, brittle, and catastrophic behaviour

The tests were performed in piston travel displacement control by setting, for all the test specimens, a velocity of 10^{-6} m/s during compression. Neutron emission measurements were made by means of a helium-3 detector placed at a distance of 10 cm from the test specimen and enclosed in a polystyrene case so as to prevent the results from being altered by vibrations or impacts. This detector was also calibrated for the measurement of thermal neutrons; its sensitivity is 65 cps/$n_{thermal}$, i.e., the flux of thermal neutrons was 1 thermal neutron/s cm^2, corresponding to a count rate of 65 cps. The neutron background was measured at 600 s time intervals to obtain sufficient statistical data. The average background count rate was: $3.8\times10^{-2}\pm0.2\times10^{-2}$ cps, corresponding to an equivalent flux of thermal neutrons of $5.8\times10^{-4}\pm0.3\times10^{-4}$ $n_{thermal}$/s cm^2.

In Fig. 6 the results obtained from one of the test specimens of Luserna Granite are presented. Neutron emissions were found to be of about one order of magnitude larger than the natural background level at the time of failure. These neutron emissions were caused by piezonuclear reactions that occurred in the granite, but did not occur in the marble.

This is due to the fact that the release rate of accumulated elastic energy ΔE exceeds the power threshold for the generation of piezonuclear reactions, as well as to the type of catastrophic failure that occurs in granite, which entails a very fast energy release, over a time interval of the order of one nanosecond [1, 2, 25].

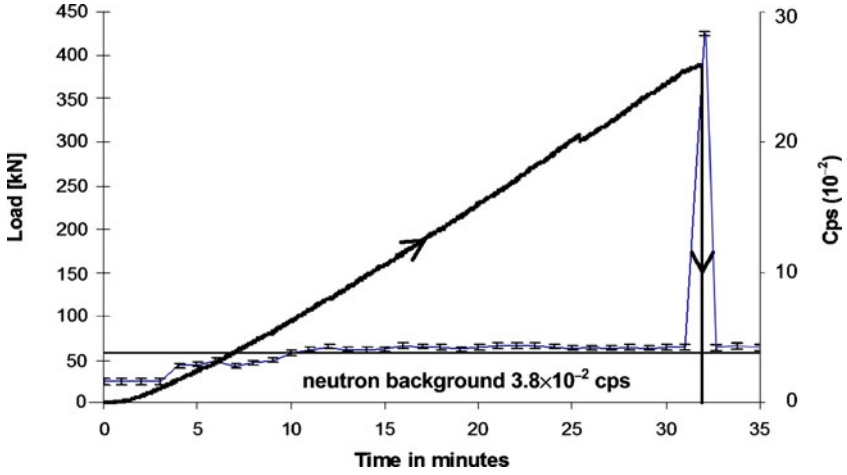

Fig. 6 Load vs. time and neutron records in counts per second (cps) for one of the Luserna Granite specimens

Another factor to be taken into account is the composition of the materials in which piezonuclear reactions may be produced. The marble used in the tests contains only iron impurities (not more than 0.07% of Fe_2O_3), and granite instead contains a considerable amount of iron (around 3% of Fe_2O_3).

This results are in strict connection with those presented in a previous contribution recently published by Cardone and co-workers [26] related to piezonuclear reactions occurring in stable iron nuclides contained in aqueous solutions of iron chloride or nitrate. In the present case, we consider a solid containing iron —samples of granite rocks— and the pressure waves in the medium are provoked by particularly brittle fracture events in compression. As ultrasounds induce cavitation in the liquids and then bubble implosion accompanied by the formation of a high-density fluid or plasma, so shock waves due to compression rupture induce a particularly sharp strain localization in the solids and then material interpenetration accompanied by an analogous formation of a high-density fluid or plasma.

Our experiment follows a different path with respect to those of other research teams, where only fissionable or light elements (deuterium) were used, in pressurized gaseous media, in fluids with ultrasounds and cavitation, as well as in solids with shock waves and fracture. We are treating with inert, stable and non-radioactive elements at the beginning of the experiments (iron), as well as after the experiments (aluminum). Neither radioactive wastes, nor gamma emissions were recorded, but only neutron emissions.

Therefore, our conjecture is that the following piezonuclear fission reaction should have occurred also in the compression tests on granite specimens [1, 2]:

$$Fe_{26}^{30} \rightarrow 2\,Al_{13}^{14} + 2 \text{ neutrons}. \quad (9)$$

Obviously we are well aware that this reaction is strongly suppressed in the framework of quantum and relativistic mechanics and in the context of a flat Minkowski's space-time. On the contrary, it is allowed, despite the fact that its probability is not yet known, according to the theory of deformed space-time [27]. In order to obtain this reaction, we must consider the boundary conditions for energy and power. About energy, we have to overcome the energy threshold $E_{0,strong}$, i.e. the limit beyond which the piezonuclear reactions are allowed, since the nuclear space-time is no longer flat. About power, we need to overcome the threshold in the "speed of energy", W_{strong}, which determines whether the potential reactions are possible or not [2].

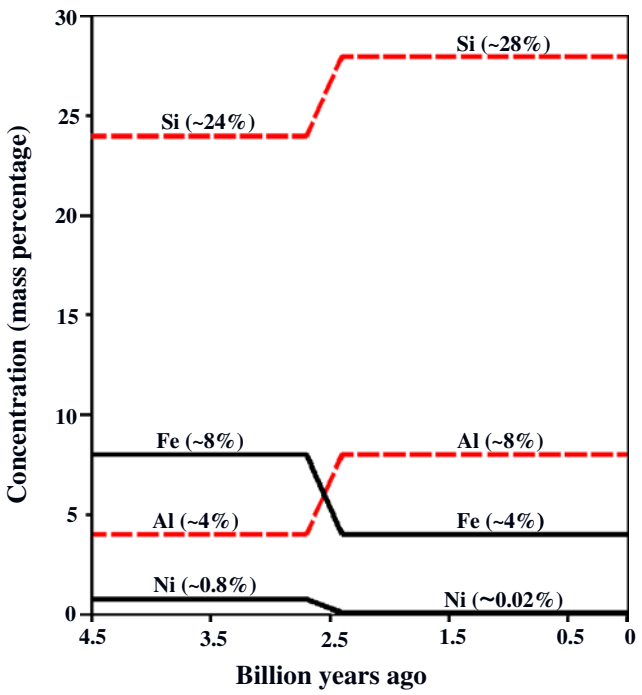

Fig. 7 Evolution in mass percentage concentration of Si, Al, Fe and Ni in the Earth crust during the last 4.5 billion of years (age of the planet Earth)

In addition to the previous observations and experiments, other strong reasons of a very general nature push us to emphasize this type of explanation. The present natural abundance of aluminum (7–8% in the Earth crust), which is less favoured than iron from a nuclear point of view (it has a lower bond energy per nucleon), is possibly due to the above piezonuclear fission reaction. This reaction —less infrequent than we could think— would be activated where the environment conditions (pressure and temperature) are particularly severe, and mechanical phenomena of fracture, crushing, fragmentation, comminution, erosion, friction, etc., may occur.

If we consider the evolution of the percentages of the most abundant elements in the Earth crust during the last 3 billion years, we realize that iron and nickel have drastically diminished, whereas aluminum, silicon and magnesium have as much increased [28–30] (Fig. 7).

It is also interesting to realize that such increases have developed mainly in the tectonic regions, where frictional phenomena between the continental plates occurred. Many other clues and quantitative data could be presented in favour of the piezonuclear fission reactions, and this will be the subject of a next publication.

Conclusions

In this paper we have considered the different forms of energy emitted during compressive failure of brittle materials. In the first part, utilizing the AE technique, the behaviour of quasi-brittle materials in compression is analysed. Such an approach, based on statistical and fractal analysis, has shown that the energy dissipation occurs over a fractal domain comprised between a surface and the material volume. We have also proposed a statistical interpretation for the variation of the *b*-value during the evolution of damage detected by AE, which is based on a treatment originally proposed by Carpinteri and co-workers [9–12]. The proposed model captures the transition from the condition of diffused damage to that of imminent failure localisation.

In the second part, we have analysed the mechanical behaviour of rocks and concrete samples loaded in compression up to their failure by the AE and EME signals. In all the considered cases, the presence of AE events has always been observed during the damage process. On the contrary, it is very interesting to note that the EME was generally observed only in correspondence to sharp stress drops in the load vs. time diagrams. These drops or "snap-back" are due to a rapid decay in the material mechanical properties, generated by the formation of new micro-cracks during the loading process [22–24].

Finally, we have investigated the piezonuclear neutron emissions from very brittle failure of rocks specimens in compression [1, 2]. As regards the neutron emission, this is the first time, at the best of authors' knowledge, that a similar phenomenon is reported to the attention of the International Scientific Community, and its discussion can be of great interest also in the field of Experimental Mechanics.

Acknowledgements The financial support provided by the Regione Piemonte RE-FRESCOS Project, is gratefully acknowledged.

Special thanks are due to A. Manuello from the Politecnico di Torino for his active collaboration in the execution of mechanical compressive tests.

The authors wish to acknowledge G. Niccolini, A. Schiavi and A. Agosto from the National Research Institute of Metrology —INRIM for previous extensive collaboration, and are also grateful to A. Zanini, L. Visca and O. Borla (INFN) for their valuable assistance with the neutron detection process.

References

1. Carpinteri A, Cardone F, Lacidogna G (2009) Piezonuclear neutrons from brittle fracture: early results of mechanical compression tests. Strain 45:332–339
2. Cardone F, Carpinteri A, Lacidogna G (2009) Piezonuclear neutrons from fracturing of inert solids. Phys Lett A 373:4158–4163
3. Ohtsu M (1996) The history and development of acoustic emission in concrete engineering. Mag Concr Res 48:321–330
4. Carpinteri A, Pugno N (2002) One- two- and three-dimensional universal laws for fragmentation due to impact and explosion. J Appl Mech 69:854–856
5. Carpinteri A, Pugno N (2004) Size effects on average and standard deviation values for the mechanical properties of condensed matter: a energy based unified approach. Int J Fract 128:253–261
6. Carpinteri A, Lacidogna G, Pugno N (2004) Scaling of energy dissipation in crushing and fragmentation: a fractal and statistical analysis based on particle size distribution. Int J Fract 129:131–139
7. Carpinteri A, Lacidogna G, Pugno N (2007) Structural damage diagnosis and life-time assessment by acoustic emission monitoring. Eng Fract Mech 74:273–289
8. Carpinteri A, Lacidogna G, Pugno N (2005) Time-scale effects during damage evolution: a fractal approach based on acoustic emission. Strength, Fracture and Complexity 3:127–135
9. Carpinteri A (1986) Mechanical Damage and Crack Growth in Concrete: Plastic Collapse to Brittle Fracture. Martinus Nijhoff, Dordrecht
10. Carpinteri A (1994) Scaling laws and renormalization groups for strength and toughness of disordered materials. Int J Solids Struct 31:291–302
11. Carpinteri A, Lacidogna G, Niccolini G, Puzzi S (2008) Critical defect size distributions in concrete structures detected by the acoustic emission technique. Meccanica 43:349–363
12. Carpinteri A, Lacidogna G, Puzzi S (2009) From criticality to final collapse: evolution of the *b*-value from 1.5 to 1.0. Chaos, Solitons & Fractals 41:843–853

13. Richter CF (1958) Elementary Seismology. W. H. Freeman & Company, San Francisco
14. Uomoto T (1987) Application of acoustic emission to the field of concrete engineering. J Acoust Emiss 6:137–144
15. Carpinteri A, Lacidogna G, Niccolini G (2005) Critical behaviour in concrete structures and damage localization by acoustic emission. Key Eng Mater 312:305–310
16. Colombo S, Main IG, Forde MC (2003) Assessing damage of reinforced concrete beam using "*b*-value" analysis of acoustic emission signals. J Mater Civ Eng, ASCE 15:280–286
17. Rundle JB, Turcotte DL, Shcherbakov R, Klein W, Sammis C (2003) Statistical physics approach to understanding the multi-scale dynamics of earthquake fault systems. Rev Geophys 41:1–30
18. Turcotte DL (1992) Fractals and chaos in geology and geophysics. Cambridge University Press, Cambridge
19. O'Keefe SG, Thiel DV (1995) A mechanism for the production of electromagnetic radiation during fracture of brittle materials. Phys Earth Plant Inter 89:127–135
20. Lacidogna G, Manuello A, Durin G, Niccolini G, Agosto A, Carpinteri A (2009) Acoustic and magnetic emissions as precursor phenomena in failure processes. *Proc. of SEM Annual Conference & Exposition on Experimental and Applied Mechanics, Albuquerque, 1–4 June 2009*. Paper No. 540
21. Schiavi A, Niccolini G, Tarizzo P, Lacidogna G, Manuello A, Carpinteri A (2009) Analysis of acoustic emission at low frequencies in brittle materials under compression. *Proc. of SEM Annual Conference & Exposition on Experimental and Applied Mechanics, Albuquerque, 1–4 June 2009*. Paper No. 539
22. Carpinteri A (1989) Cusp catastrophe interpretation of fracture instability. J Mech Phys Solids 37:567–582
23. Carpinteri A (1990) A catastrophe theory approach to fracture mechanics. Int J Fract 44:57–69
24. Hudson JA, Crouch SL, Fairhurst C (1972) Soft, stiff and servo-controlled testing machines: a review with reference to rock failure. Eng Geol 6:155–189
25. Carpinteri A, Corrado M (2009) An extended (fractal) overlapping crack model to describe crushing size-scale effects in compression. Eng Fail Anal 16:2530–2540
26. Cardone F, Cherubini G, Petrucci A (2009) Piezonuclear neutrons. Phys Lett A 373:862–866
27. Cardone F, Mignani R (2007) Deformed spacetime. Springer, Dordrecht, Chaps 16–17
28. Anbar AD (2008) Elements and evolution. Science 322:1481–1482
29. Favero G, Jobstraibizer P (1996) The distribution of aluminum in the Earth: from cosmogenesis to Sial evolution. Coord Chem Rev 149:467–400
30. Konhauser KO, Pecoits E, Lalonde SV, Papineau D, Nisbet EG, Barley ME, Arndt NT, Zahnle K, Kamber BS (2009) Oceanic Nickel depletion and a methanogen famine before the great oxidation event. Nature 458:750–754